Characteristics of starch-based films plasticised by glycerol and by the ionic liquid 1-ethyl-3-methylimidazolium acetate: a comparative study

Fengwei Xie [a,*], Bernadine M. Flanagan [b], Ming Li [b], Parveen Sangwan [c], Rowan W. Truss [d], Peter J. Halley [a,d], Ekaterina V. Strounina [e], Andrew K. Whittaker [a,e,] Michael J. Gidley [b], Katherine M. Dean [c], Julia L. Shamshina [f], Robin D. Rogers [f], Tony McNally [g]

[a] *Australian Institute for Bioengineering and Nanotechnology, The University of Queensland, Brisbane, Qld 4072, Australia*

[b] *Centre for Nutrition and Food Sciences, Queensland Alliance for Agriculture and Food Innovation, The University of Queensland, Hartley Teakle Building, St Lucia, Queensland 4072, Australia*

[c] *CSIRO Materials Science and Engineering, Gate 5 Normanby Rd, Clayton, Vic 3168, Australia*

[d] *School of Chemical Engineering, The University of Queensland, Brisbane, Qld 4072, Australia*

[e] *Centre for Advanced Imaging, The University of Queensland, Brisbane, Qld 4072, Australia*

[f] *Center for Green Manufacturing and Department of Chemistry, The University of Alabama, Tuscaloosa, AL 35487, USA*

[g] *WMG, University of Warwick, CV4 7AL, UK*

[*] Corresponding author. Tel.: +61 7 3346 3199; fax: +61 7 3346 3973.

Email address: f.xie@uq.edu.au; fwhsieh@gmail.com (F. Xie)

ABSTRACT

This paper reports the plasticisation effect of the ionic liquid, 1-ethyl-3-methylimidazolium acetate ([Emim][OAc]), as compared with the traditionally used plasticiser, glycerol, on the characteristics of starch-based films. For minimising the additional effect of processing, a simple compression moulding process (which involves minimal shear) was used for preparation of starch-based films. The results show that [Emim][OAc] was favourable for plasticisation, i.e., disruption of starch granules (by scanning electron microscopy), and could result in a more amorphous structure in the starch-based materials (by X-ray diffraction and dynamic mechanical analysis). ^{13}C CP/MAS and SPE/MAS NMR spectroscopy revealed that not only was the crystallinity reduced by [Emim][OAc], but also the amorphous starch present was plasticised to a more mobile form as indicated by the appearance of amorphous starch in the SPE/MAS spectrum. Mechanical results illustrate that, when either glycerol or [Emim][OAc] was used, a higher plasticiser content could contribute to higher flexibility. In spite of the accelerated thermal degradation of starch by [Emim][OAc] as shown by thermogravimetric analysis, the biodegradation study revealed the antimicrobial effect of [Emim][OAc] on the starch-based materials. Considering the high-amylose starch used here which is typically difficult to gelatinise in a traditional plasticiser (water and/or glycerol), [Emim][OAc] is demonstrated to be a promising plasticiser for starch to develop "green" flexible antimicrobial materials for novel applications.

Keywords:

Starch; Ionic liquid; 1-ethyl-3-methylimidazolium acetate; Plasticization; Crystalline structure; Biodegradability

Chemical compounds studied in this article

Starch (PubChem CID: 24836924); Water (PubChem CID: 962); Glycerol (PubChem CID: 753); 1-Ethyl-3-methylimidazolium acetate (PubChem CID: 11658353)

1. Introduction

In recent years, polymers from renewable resources have attracted great attention due to their availability, renewability, biocompatibility, and biodegradability (Yu, Dean, & Li, 2006). Starch, among this group of polymers, can be processed with conventional processing techniques such as compression moulding, extrusion, and injection moulding and is therefore considered as an important alternative to traditional non-renewable, non-biodegradable petroleum-based polymers (Liu, Xie, Yu, Chen, & Li, 2009; Xie, Halley, & Avérous, 2012; Xie, Liu, & Yu, 2014).

Starch, nonetheless, has unique characteristics naturally: in plants, it exists in the form of granules (<1 μm~100 μm); the granule is composed of alternating amorphous and semicrystalline shells (growth rings) (100~400 nm); and the semicrystalline shell is stacked by crystalline and amorphous lamellae (periodicity, 9~10 nm); while starch consists of two major biomacromolecules called amylose (mainly linear) and amylopectin (hyper-branched) (~nm) (Fu, Wang, Li, Wei, & Adhikari, 2011; Jane, 2009; Pérez, Baldwin, & Gallant, 2009; Pérez, & Bertoft, 2010). The 3D structure of native starch may be disrupted with a plasticiser and elevated temperature, a process known as "gelatinisation" or "melting". If suitable conditions are reached, this results in a homogeneous amorphous material known as "thermoplastic starch" or "plasticised starch", which is the essential principle in starch processing (Avérous, 2004; Liu et al., 2009). While water is the most commonly used and effective plasticiser for starch, many other substances have been used to plasticise starch, such as polyols (glycerol, glycol, sorbitol, etc.), compounds containing nitrogen (urea, ammonium derived chemicals, amines), and citric

acid (Liu et al., 2009; Xie et al., 2012). Favourable attributes of a plasticiser for starch include being stable (non-volatile) both during thermal processing and in the post-processing stages, having little effect on starch macromolecular degradation, being safe to humans and environmentally friendly, and being advantageous for reducing the inherent hydrophilicity of starch and for long-term stability. Unfortunately, plasticisers such as some of those mentioned above rarely meet all the attributes and therefore finding a better plasticiser for starch is of interest.

Ionic liquids (ILs), now commonly defined as salts which melt below 100 °C, have recently attracted much interest for aiding the processing of biopolymers like starch. Many ILs, especially ones based on the imidazolium cation, have been shown to be capable of dissolving polysaccharides such as starch and thus can be used as an excellent media for polysaccharide plasticisation and modification (Biswas, Shogren, Stevenson, Willett, & Bhowmik, 2006; El Seoud, Koschella, Fidale, Dorn, & Heinze, 2007; Wilpiszewska, & Spychaj, 2011; Zakrzewska, Bogel-Łukasik, & Bogel-Łukasik, 2010). Moreover, the use of ILs could also allow the development of starch-based ionically conducting polymers or solid polymer electrolytes (Liew, Ramesh, Ramesh, & Arof, 2012; Ramesh, Liew, & Arof, 2011; Ramesh, Shanti, Morris, & Durairaj, 2011; Ramesh, Shanti, & Morris, 2012; Wang, Zhang, Liu, & He, 2009; Wang, Zhang, Wang, & Liu, 2009; Wang, Zhang, Liu, & Han, 2010b). Nevertheless, most of the work done before in this area involved the processing in solution, although melt processing is seen to be more suitable for industrial production as much less solvent is required and higher efficiency is expected. Sankri et al. (2010) and Leroy, Jacquet, Coativy, Reguerre, and Lourdin (2012) have done pioneering work using an IL (1-butyl-3-methylimidazolium chloride) as a new plasticiser in melt processing of starch-based materials where improvements in plasticisation, electrical conductivity, and hydrophobicity were demonstrated.

This paper reports the preparation by a simple one-step compression moulding process of IL–plasticised starch-based films, which are compared with glycerol-plasticised starch-based films. It is noted that many of the ILs used previously with starch contained the corrosive [Cl^-] anion (e.g., 1-butyl-3-methylimidazolium chloride) (Wilpiszewska, & Spychaj, 2011) and this type of IL could contribute to macromolecular degradation of starch (Kärkkäinen, Lappalainen, Joensuu, & Lajunen, 2011; Stevenson, Biswas, Jane, & Inglett, 2007), resulting from the acidic hydrolysis of glycosidic bonds in starch-based materials, due to the formation of HCl. Therefore, 1-ethyl-3-methylimidazolium acetate ([Emim][OAc]), an IL with a non-halogen-containing, weaker acid, anion, was chosen in the current work. [Emim][OAc] has very low vapour pressure, high thermal stability, and relatively low viscosity at room temperature (Liu, & Budtova, 2012), which enables it to be used with starch in a wide range of processing conditions. Our recent finding (Mateyawa et al., 2013) has shown that the best plasticisation of starch may be achieved once a certain ratio of water/[Emim][OAc] is met. In the current study, this effect of water/[Emim][OAc] ratio was also used, and the plasticiser effects on the morphology, crystalline structure, mechanical properties, glass transition temperature, thermal stability, and biodegradability of the starch-based films are thus reported, which provides valuable information for understanding the starch–IL interactions and for designing starch-based materials with desired properties. While in extrusion or kneading different formulation can change the viscosity and cause different degrees of shear degradation of starch macromolecules, which alters the final properties, a simple compression moulding method is used here to minimise the effect of shear-induced macromolecular degradation during processing.

2. Materials and Methods

2.1. Materials

A commercially available maize starch, Gelose 80, was used in this work, which was supplied by Ingredion ANZ Pty Ltd (Lane Cove, NSW, Australia). It was chemically unmodified and the amylose content was 82.9% as measured before (Tan, Flanagan, Halley, Whittaker, & Gidley, 2007). The original moisture content of the starch was 14.4 wt.%. Deionised water was used in all instances. Glycerol (AR) was supplied by Chem-Supply Pty Ltd (Gillman, SA, Australia) and was used as received. [Emim][OAc] of purity ≥95%, produced by IoLiTec Ionic Liquids Technologies GmbH (Salzstraβe 184, D-74076 Heilbronn, Germany), was supplied by Chem-Supply Pty Ltd as well. [Emim][OAc] was used as received. As [Emim][OAc] was in liquid form at room temperature, different weight ratios of water–[Emim][OAc] mixture could be easily prepared in vials for subsequent usage. Water and [Emim][OAc] were completely miscible as shown in our previous study (Mateyawa et al., 2013).

2.2. Sample preparation

Formulations for sample preparation are shown in Table 1. In Table 1 and the following text, the plasticised starch samples are coded in the format of "G18" or "I18", where "G" denotes glycerol and "I" the ionic liquid, and the number stands for the content of the plasticiser (either glycerol or ionic liquid). Water was used with the plasticiser and the liquid mixture (either water–glycerol or water–[Emim][OAc]) content was fixed at 30 wt.% based on our preliminary trials. The liquid mixture was added dropwise into starch, accompanied by careful blending by using a mortar and a pestle to ensure the uniform distribution of the liquid in starch. Then, the blended samples were hermetically stored in ziplock bags in a refrigerator (4 °C) at least overnight before compression moulding. This allowed a further equilibration process for the samples. The powder was carefully and evenly spread onto the

moulding area with polytetrafluoroethylene glass cloths (Dotmar EPP Pty Ltd, Acacia Ridge, Qld, Australia) located between the starch and the mould, and then compression moulding was carried out at 160 °C and 6 MPa for 10 min, followed by rapidly cooling to room temperature with circulation of water before opening the mould and collecting the sample. All the samples were conditioned at 52% relative humidity by placing them in a desiccator with saturated magnesium nitrate solution at room temperature for one month before any characterisation work.

[Insert Table 1 here]

2.3. Characterisation

2.3.1. Scanning electron microscopy (SEM)

The starch samples were cryo-ground in liquid nitrogen and then put on circular metal stubs previously covered with double-sided adhesive before platinum coating at 5 nm thickness using an Eiko Sputter Coater, under vacuum. The morphology of the starch samples was examined using a scanning electron microscope (SEM, JEOL XL30, Tokyo, Japan). An accelerating voltage of 3 kV and spot size of 6 nm were used.

2.3.2. X-ray diffraction (XRD)

The starch samples were placed in the sample holder of a powder X-ray diffractometer (D8 Advance, Bruker, Madison, USA) equipped with a graphite monochromator, a copper target, and a scintillation counter detector. XRD patterns were recorded for an angular range (2θ) of 3–40°, with a step size of

0.02° and a step rate of 0.5 s per step, and thus the scan time lasted for approximately 15 min. The radiation parameters were set as 40 kV and 30 mA, with a slit of 2 mm. Traces were processed using the Diffracplus Evaluation Package (Version 11.0, Bruker, Madison, USA) to determine the X-ray diffractograms of the samples. The degree of crystallinity was calculated using the method of Lopez-Rubio, Flanagan, Gilbert, and Gidley (2008) with the PeakFit software program (Version 4.12, Systat Software, Inc. San Jose, USA), using Equation 1:

$$X_c = \frac{\sum_{i=1}^{n} A_{ci}}{A_t} \quad (1)$$

where A_{ci} is the area under each crystalline peak with index i, and A_t is the total area (both amorphous background and crystalline peaks) under the diffractogram.

The V-type crystallinity (the crystalline amylose-lipid complex) was calculated based on the total crystalline peak areas at 7.5, 13, 20, and 23° (van Soest, Hulleman, de Wit, & Vliegenthart, 1996).

2.3.3. Nuclear magnetic resonance (NMR)

The rigid components of the starch-based films were examined by solid-state ^{13}C cross-polarization magic angle spinning nuclear magnetic resonance (^{13}C CP/MAS NMR) experiments at a ^{13}C frequency of 75.46 MHz on a Bruker MSL-300 spectrometer. Using scissors, the sheets were cut into small evenly sized pieces and were packed in a 4-mm diameter, cylindrical, PSZ (partially-stabilized zirconium oxide) rotor with a KelF end cap. The rotor was spun at 5 kHz at the magic angle (54.7°). The 90° pulse width was 5 μs and a contact time of 1 ms was used for all samples with a recycle delay of 3 s. The spectral width was 38 kHz, acquisition time 50 ms, time domain points 2 k, transform size 4 k, and line broadening 50 Hz. At least 2400 scans were accumulated for each spectrum. Spectra were referenced to external adamantane. Spectra were analysed by resolving the spectra into ordered and amorphous

subspectra and calculating the relative areas as described previously (Tan et al., 2007). To examine the mobile components of the samples, single pulse excitation, direct polarization (^{13}C SPE/MAS NMR) was used as well. The recycle time was 60 s and 20 k spectra were accumulated.

2.3.4. Tensile testing

Tensile tests were performed with an Instron® 5543 universal testing machine (Instron Pty Ltd, Bayswater, Vic., Australia) on dumbbell-shaped specimens cut from the sheets with a constant deformation rate of 10 mm/min at room temperature. The specimens corresponded to the Type 4 of the Australian Standard AS 1683:11 (ISO 37:1994), and briefly the testing section of the specimen was 12 mm in length and 2 mm in width. Young's modulus (E), tensile strength (σ_t), and elongation at break (ε_b) were determined by the Instron® computer software program, from at least 7 specimens for each of the plasticised starch sample.

2.3.5. Dynamic mechanical thermal analysis (DMTA)

Dynamic mechanical thermal analysis (DMTA) was performed on the rectangular tensile bars of the plasticised starch samples by using a Rheometric Scientific™ DMTA IV machine (Rheometric Scientific, Inc., Piscataway, NJ, USA) with the dual cantilever bending mode from −100 to 110 °C, with a heating rate of 3 °C/min, a frequency of 1 Hz, and a strain value of 0.05%. The dynamic storage modulus (E'), loss modulus (E''), and loss tangent ($\tan \delta = E''/E'$) were obtained from the tests. To prevent water evaporation during the tests, the specimens were coated with Vaseline grease. No swelling of the specimens was observed, suggesting no adverse effect of Vaseline.

197 *2.3.6. Thermogravimetric analysis (TGA)*

198 A Mettler Toledo TGA/DSC1 thermogravimetric analyser was used with 40 μL aluminium crucibles.
199 A sample mass of about 5 mg was used for each run. The samples were heated from 25 °C to 550 °C at
200 3 °C/min under nitrogen environment.

201

202 *2.3.7. Biodegradation*

203 The biodegradability of the starch samples was determined according to the Australian Standard AS
204 ISO 14855. The test material was reduced in size to achieve maximum surface area of each individual
205 piece of the test material, approximately 2 cm × 2 cm. Each composting vessel contained 100 g of the
206 test material and 600 g of the compost inoculum, both on dry weight basis. Each material was tested in
207 triplicate including the blank (the compost only) and positive (a mixture of cellulose and the compost)
208 references. All composting vessels were then placed inside an in-house built respirometer unit (Way,
209 Wu, Dean, & Palombo, 2010) and the temperature was maintained at 58±2 °C for all the testing period.
210 During this degradation period, the compost moisture content was maintained at 48–50% and the pH at
211 7.8–8.5 to ensure favourable conditions for the compost microorganisms involved in the biodegradation
212 process. Aerobic conditions were maintained by continuous supply of sufficient airflow to the
213 bioreactors and the contents of each of the bioreactors were mixed once a week to ensure uniform
214 distribution of air throughout the compost. The evolved CO_2 and flow rate data were continually data-
215 logged by computer for each respective bioreactor. The theoretical amounts of CO_2 produced by the test
216 and reference materials were assessed and the degree of biodegradation, D_t, was calculated (for the test
217 and reference materials) using the following equation, as described in the Australian Standard AS ISO
218 14855:

219 $$D_t = \frac{(CO_2)_T - (CO_2)_B}{THCO_2} x100 \qquad (2)$$

where $(CO_2)_T$ is the cumulative amount of carbon dioxide evolved in each bioreactor containing the test material (in grams per bioreactor), and $(CO_2)_B$ is the mean cumulative amount of carbon dioxide evolved in the blank vessel (in grams per bioreactor).

3. Results and Discussion

3.1. Morphology

In order to understand the morphology of the samples after processing, SEM work was carried out and the images are shown in Figure 1. Different kinds of morphology are shown by the different samples. From the normal surface images, a higher amount of glycerol could result in a more apparent granular morphology. In particular, most remaining starch granules could be observed as contained in G27, while G9 showed a smooth surface. This was reasonable as the use of glycerol instead of water should increase the gelatinisation temperature, in other words making gelatinisation more difficult (Liu et al., 2011). Among the [Emim][OAc]-plasticised samples, I18 seemed to have the most granular surface, which however was still less granular than G27. These results demonstrate a stronger effect of [Emim][OAc] on the disruption of granules during processing. This is especially true noting that in this study only a simple compression moulding process was used which involved little shear and Gelose 80 (a high-amylose content starch) was used which, though is desirable for producing films with better properties, is known to have poor processibility due to the difficulty in granule disruption (Li et al., 2011; Wang et al., 2010a).

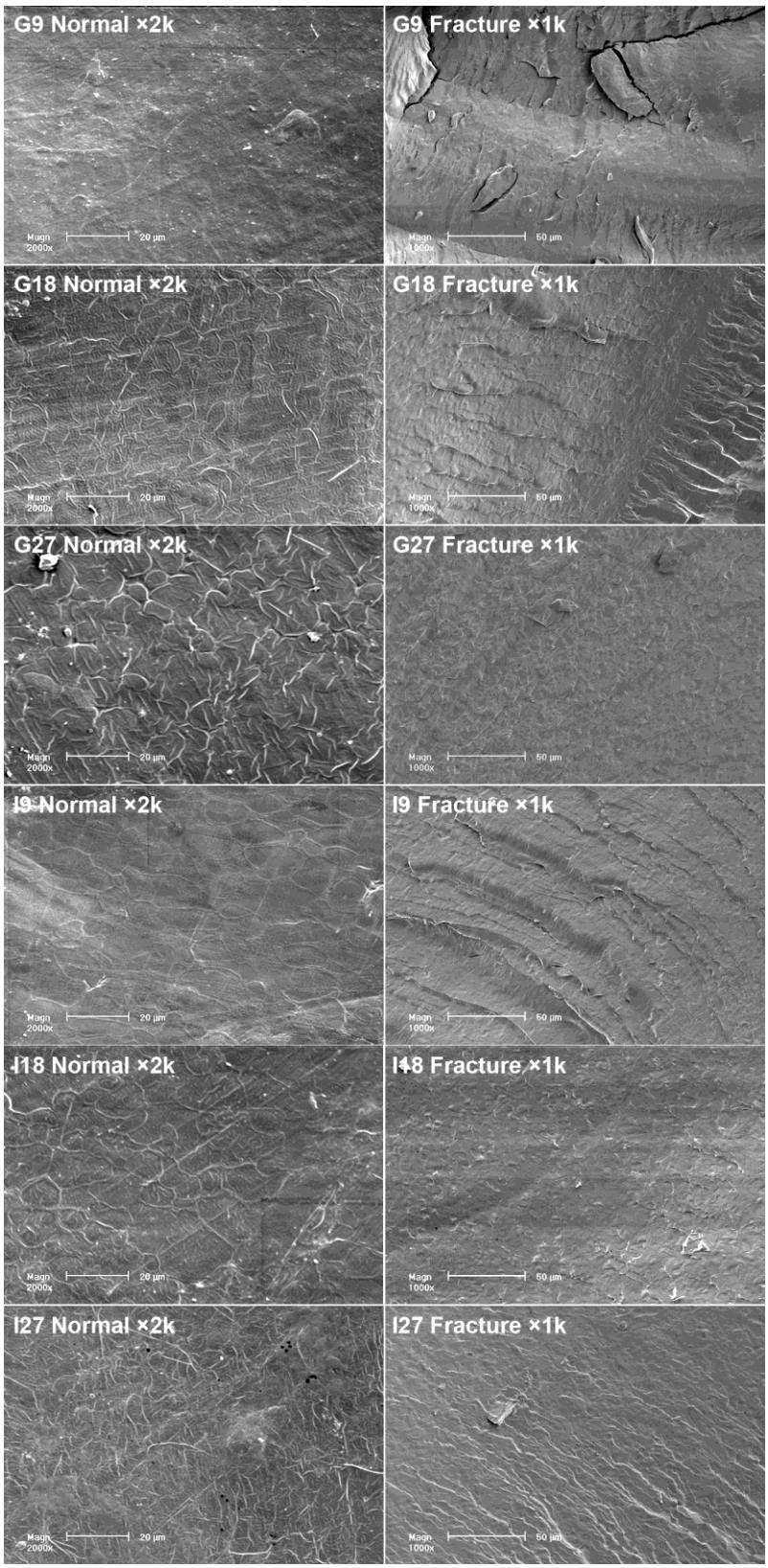

241

242 Figure 1 SEM images of both normal and fracture surfaces of the different starch samples.

The fracture surface images in Figure 1 show that the samples with lower content of the plasticiser (either glycerol or [Emim][OAc]) appeared to be more brittle, which was as expected as plasticisers generally make polymers more ductile. G9 seemed to be more brittle than I9, again showing a better plasticisation effect of [Emim][OAc] than that of glycerol. This property will be further shown later in the mechanical results.

3.2. XRD and NMR analyses

Figure 2 shows the XRD patterns of native Gelose 80 starch and the different starch samples. The native starch showed the strongest diffraction peaks at 2θ of around 17°, with a few smaller peaks at 2θ of around 5°, 10°, 14°, 15°, 19°, 22°, 23°, 26°, 31°, and 34°, which were indicative of the B-type crystalline structure (Cheetham, & Tao, 1998; Lopez-Rubio et al., 2008). After processing, in addition to the original B-type characteristic peaks (main peak at 2θ = 17.1°), all the starch samples displayed peaks at 2θ of around 7°, 13°, 20°, and 22°, which were characteristic of the V_H-type crystalline structure, a single-helical amylose structure. This is similar to the one formed by amylose–lipid helical complexes which is well known for thermally processed (by e.g. compression moulding and extrusion) starch-based materials (van Soest et al., 1996). In other words, the plasticised samples contained some crystalline structures that were not destroyed by the compression moulding process and some newly formed V-type crystalline structures mainly induced by the processing.

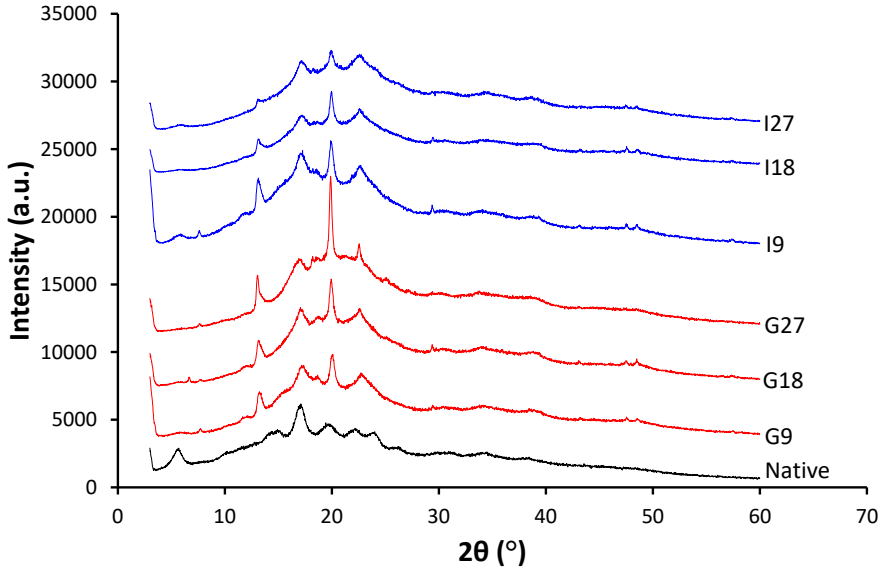

Figure 2 XRD patterns of native starch (Gelose 80) and the different starch samples.

Table 1 also shows the crystallinity of the samples calculated from the XRD results. For the glycerol-plasticised samples, an increase in the glycerol content resulted in an increase in the intensity of 2θ peak at 20° (the V-type crystallinity increased from 5.5% to 6.8% with the increased content of glycerol from 9% to 27%), suggesting that glycerol could promote the formation of the single-helical amylose structure. However, the B-type crystallinity largely decreased (from 26.6% to 13.9%) with a higher glycerol content, resulting in a decrease in the total crystallinity (from 32.1% to 20.7%). Along with the previous morphological results, it is interesting to summarise that a higher glycerol content (less water content) could result in more granule remains but less B-type crystallinity with the processing method used in this study.

On the other hand, for the [Emim][OAc]-plasticised samples, an increase in the [Emim][OAc] content contributed to a decrease in both the B-type crystallinity and the V-type crystallinity and thus a decrease in the total crystallinity. As observed for the glycerol-plasticised samples, a higher water

281 content (lower [Emim][OAc] content) resulted in less complete melting of granular crystallites. Unlike
282 glycerol, the use of [Emim][OAc] seemed to be able to hinder the formation of the single-helical
283 structure. Single helices of starch are formed via hydrogen bonding between the O3' and O2 oxygen
284 atoms of sequential residues. Additionally, a helical amylose has hydrogen-bonding O2 and O6 atoms
285 on the outside surface of the helix, forming a double-helical structure via hydrogen bonding of two
286 strand-adjacent glucose molecules and holding the two strands of the double helix together. It is
287 proposed that the effect of hindering either helix formation is due to the strong interaction between
288 acetate anion in [Emim][OAc] and starch hydroxyl groups, disrupting hydrogen bonding in the starch
289 polymer and making it difficult for the amylose molecules to form single (and double) helices. The fact
290 that [Emim][OAc]-plasticised starch has low crystallinity can be beneficial to the production of
291 electrically conductive materials which need to be essentially amorphous.
292 When the XRD data of starch granule are fitted using the crystal-defect method (Lopez-Rubio et al.,
293 2008), there is usually a close agreement between the crystallinity values from XRD and from ^{13}C
294 CP/MAS NMR. However, in the presence of a plasticiser, analysis of the ^{13}C CP/MAS spectra reveals
295 highly ordered sub-spectra and the percentages of amorphous starch are much lower than the values
296 found from XRD analysis. A similar effect is observed when starch is hydrated, the amorphous starch
297 becomes more mobile and is no longer observed in the ^{13}C CP/MAS spectrum as the cross-polarization
298 efficiency is reduced (Bogracheva, Wang, & Hedley, 2001; Colquhoun, Parker, Ring, Sun, & Tang,
299 1995; Tang, & Hills, 2003; Veregin, Fyfe, Marchessault, & Taylor, 1986).
300 To examine the mobile elements of the starch sheets, ^{13}C SPE/MAS spectra were recorded, which
301 revealed the presence of amorphous starch as shown in Figure 3. To calculate the amount of mobile
302 amorphous starch, it was assumed that all the crystalline starch was described by the XRD crystal-defect
303 fitting. Then, the difference in the percentage between amorphous starch calculated from XRD and that

from ^{13}C CP/MAS was considered to be due to the mobile amorphous starch. Table 1 shows that as the amount of [Emim][OAc] increased, the degree of crystallinity decreased in much the same way as for glycerol but the mobility of the amorphous starch was greatly increased indicating that the starch was more plasticised.

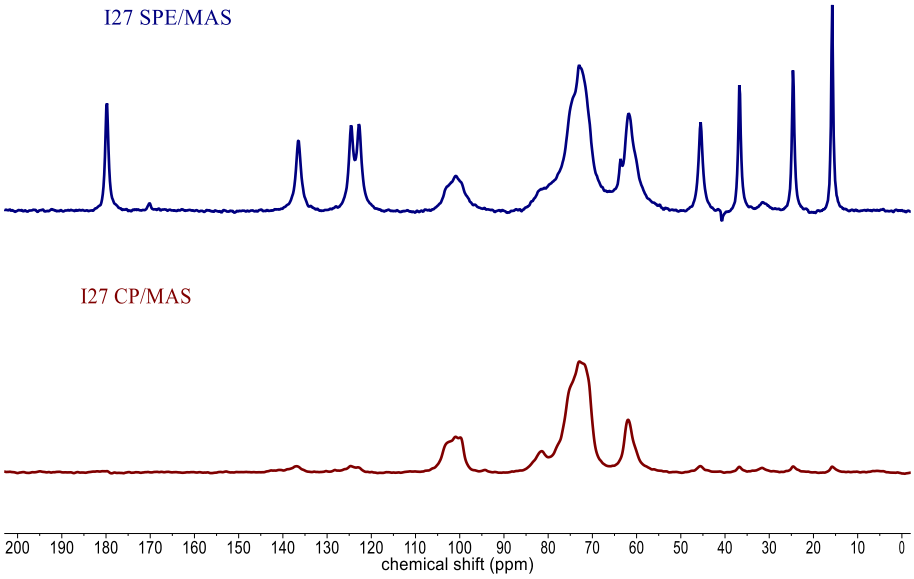

Figure 3 ^{13}C CP/MAS and SPE/MAS NMR spectra of the sample I27 revealing the presence of [Emim][OAc] and amorphous starch in the SPE/MAS spectrum and the highly ordered material in the CP/MAS spectrum.

3.3. Mechanical properties

Figure 4 shows the tensile properties of the different starch samples. Both glycerol and [Emim][OAc] impacted on the tensile properties in the same way. It can be seen that the sample with a

lower plasticiser (either glycerol or [Emim][OAc]) content had a higher tensile strength (σ_t). Comparing the samples with the different plasticisers, I9 had the same tensile strength as G9, while I18 and I27 have similar or slightly lower tensile strength than G18 and G27, respectively. The modulus (E) values showed the same trends as for σ_t. G9 or I9 showed the lowest elongation at break (ε_b) while G18 or I18 had the highest (30%). These results confirmed the brittle nature of fracture surfaces of G9 and I9. With a further increase in the plasticiser content from 18% to 27%, the plasticisation effect decreased the ε_b. This could be because when the material became too soft by the plasticiser there was no work hardening to stabilise drawing; this could also be ascribed to possible phase separation when the plasticiser content was too high. Taking into account of the high variance of ε_b, the overall trend of the mechanical property data was that [Emim][OAc] provided similar or perhaps slightly better plasticisation effects than glycerol.

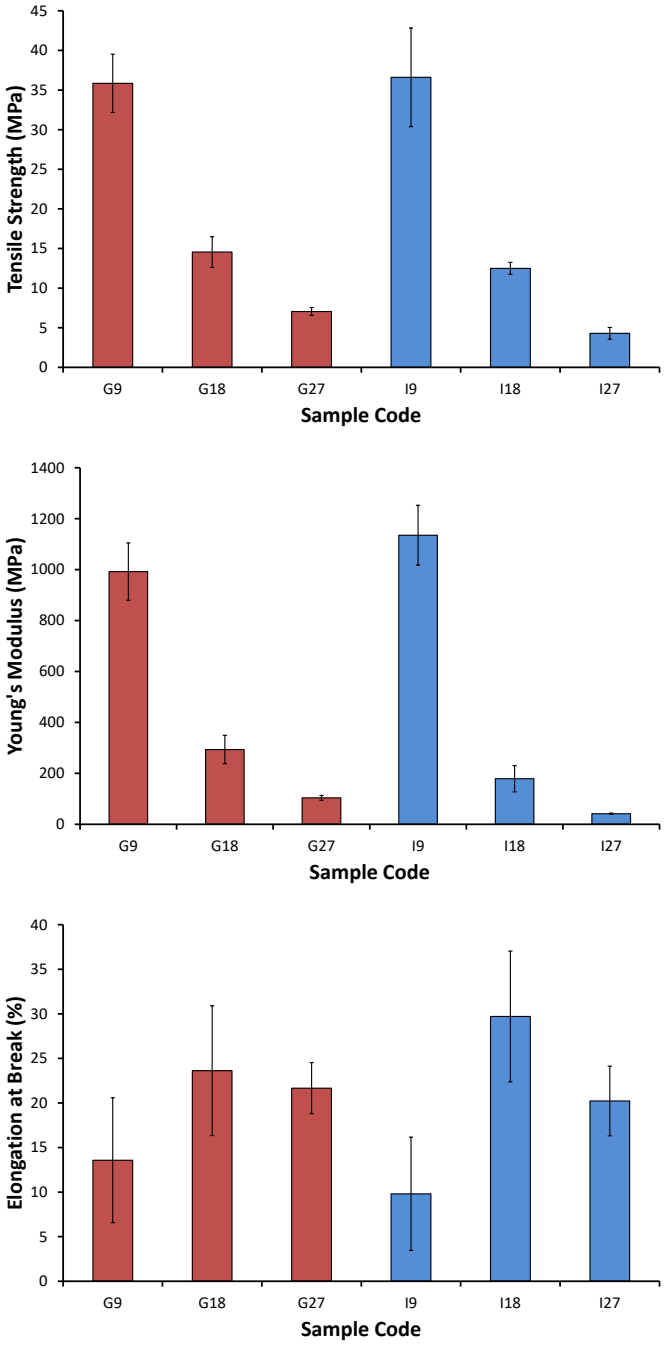

332

333 Figure 4 Tensile strength (σ) (top), Young's modulus (middle), and elongation at break (ε_b) (bottom) of

334 the different starch samples. The errors bars represent standard deviations.

335

336

Mechanical properties can be affected by various factors such as the plasticiser type and content, granule remains in the matrix, the crystalline structure and crystallinity, and the extent of plasticisation of the amorphous parts. The highest σ_t and E, and the lowest ε_b of G9 or I9 could be mainly attributed to the less melting of original granule crystallites. Noting the highest ε_b values of G18 and I18, it is suggested that the large amount of mobile amorphous phase contributed by the plasticiser (cf. XRD and NMR results) could be the reason. However, when the [Emim][OAc] content was even higher, the material (G27 and I27) became too soft (as discussed above) so the ε_b value was reduced.

3.4. DMTA analysis

Figure 5 shows the DMTA results of the different starch samples. For some of the samples, a prominent peak was shown between 30 °C and 100 °C. Based on previous studies (Madrigal, Sandoval, & Müller, 2011; Perdomo et al., 2009), this peak can be undoubtedly attributed to the glass transition of starch (T_g), which will be the main focus discussed below; at a lower temperature, another peak might be shown which can be ascribed to the glass transition of the plasticiser-rich domains.

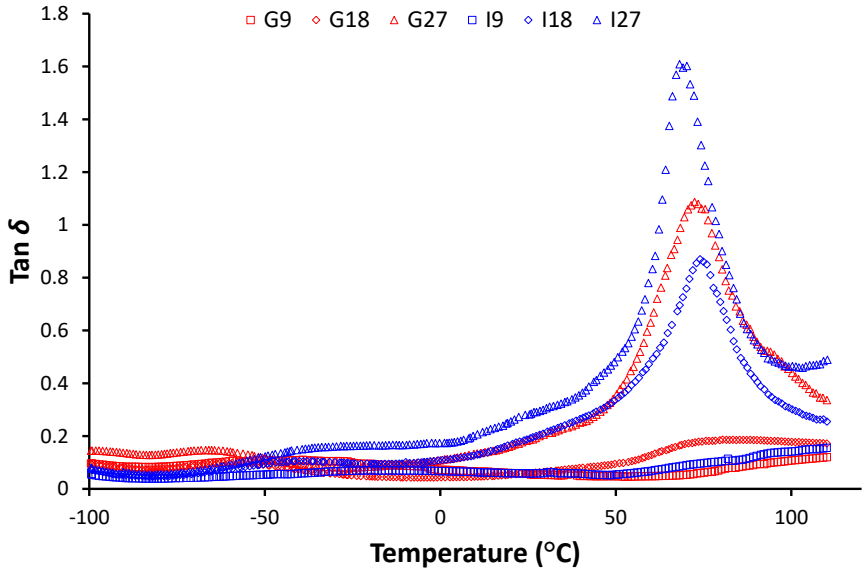

Figure 5 Tan δ results of the different starch samples.

It can be seen that, while the T_g could hardly be seen for G9 or I9, a higher plasticiser content contributed to a more prominent peak representing the starch glass transition. Compared to glycerol, the use of [Emim][OAc] as the plasticiser gave a stronger glass transition peak and the peak temperature was lower. For example, the T_g of I27 was 68.2 °C while that of G27 was 71.5 °C. This phenomenon shows that both a higher content of the plasticiser and the use of [Emim][OAc] instead of glycerol resulted in less crystallinity as well as more amorphous structure which was more mobile, which is in good agreement with the XRD and NMR results.

3.5. TGA

Figure 6 shows the TGA results of the different starch samples, in terms of both percentage of weight loss and its derivative value. The results clearly suggest that with use of [Emim][OAc], thermal degradation happened at a lower temperature. Judging from the peak temperature of the derivative

weight percentage, I27 had a thermal degradation temperature of 266 °C, which is 30 °C lower than that of G27. While no reports have been released regarding the TGA of ionic liquid-plasticised starch-based materials, previously studies have shown that ionic liquid has an effect of reducing the molecular weight of starch during solution processing with heat (Kärkkäinen et al., 2011; Stevenson et al., 2007). It is thus proposed that the existence of [Emim][OAc] could promote the thermal degradation of starch molecules.

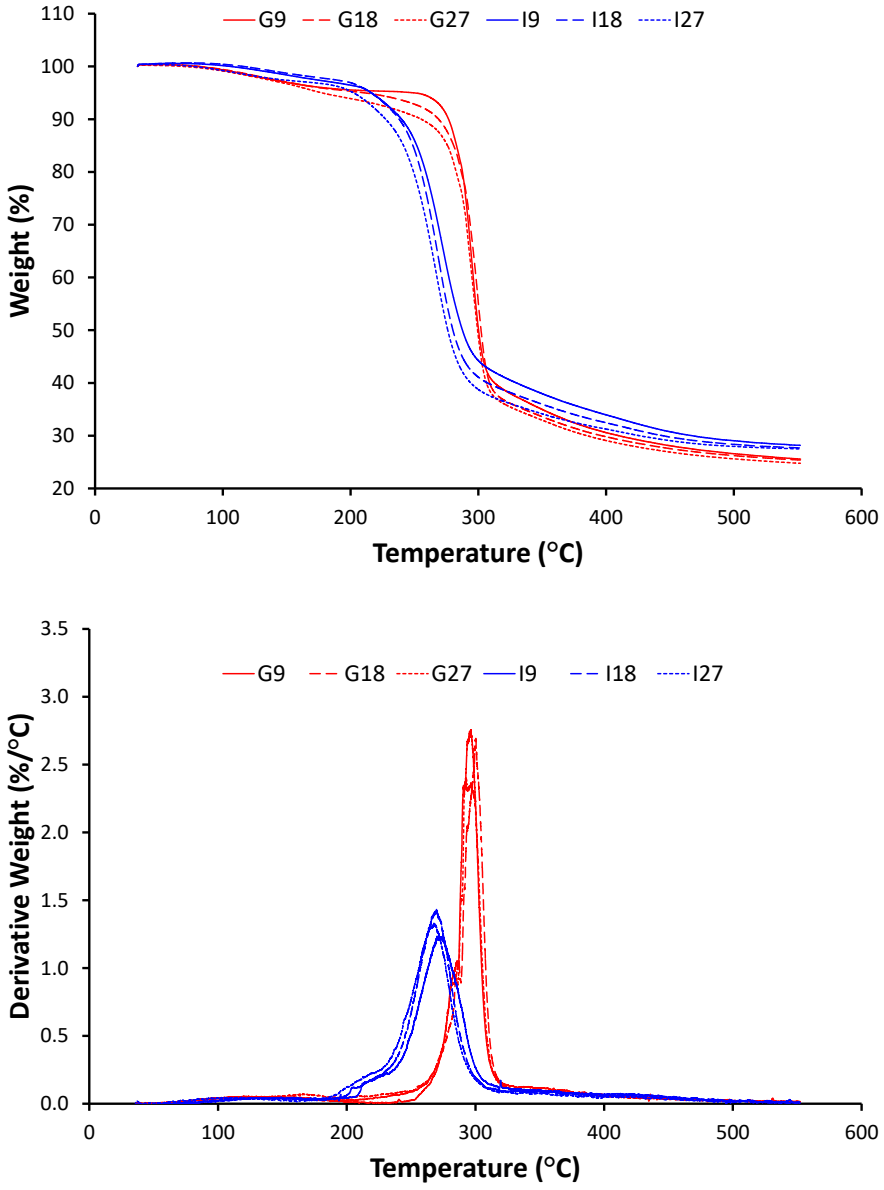

Figure 6 TGA results in terms of weight percentage (a) and derivative weight percentage (b) of the different starch samples.

3.6. Biodegradation

Table 1 also shows the biodegradation results after 1, 2, and 3 month(s) of aerobic composting. It can be clearly seen that there is a big difference between the glycerol-plasticised samples and the ionic

liquid-plasticised samples: the former experienced much greater biodegradation than the latter. For all glycerol-plasticised samples, the biodegradation percentages were over 50%, and increased with time; in contrast, the 1-month results for I9, I18, and I27 were just 34%, 14%, and 17%, respectively, which increased only slightly over another two months. Along with the morphological and crystalline structure results, it is apparent that the plasticiser played a dominant role in biodegradation, whilst the effect of crystalline structure was minor. [Emim][OAc] seemed to be able to inhibit the attack of bacteria to starch. While this has not been reported yet, the literature has already shown the antibacterial activity of some other ionic liquids (Thuy Pham, Cho, & Yun, 2010). The mechanism regarding the antibacterial effect of [Emim][OAc] needs further investigation. Nevertheless, the results here provide us a promising way for developing antimicrobial starch-based materials with ILs.

4. Conclusion

In this study, the plasticisation effect of [Emim][OAc], as compared with glycerol, which is the most commonly used plasticiser for starch, on the characteristics of starch-based films was investigated. Despite choosing a high-amylose starch, Gelose 80, which is known to have difficulty in granule disruption and poor processibility, [Emim][OAc] was shown to be effective in plasticisation of this starch although only a compression moulding process involving little shear treatment was employed. Compared with glycerol, [Emim][OAc] contributed to less granule remains as observed by SEM. The XRD and NMR results reveal that [Emim][OAc] at a low concentration disrupted the original B-type crystalline structure, generated less V-type crystalline structure, and increased the mobility of the amorphous starch. As a result, a highly amorphous structure contributed to higher flexibility as shown by mechanical tests and a lower glass transition temperature but stronger glass transition peak as revealed by DMTA. Although the TGA results show the accelerated thermal degradation of starch by

[Emim][OAc] as compared with glycerol, the biodegradation study reveals that [Emim][OAc] inhibited bacterial attack to the starch-based materials. However, [Emim][OAc] could be a promising plasticiser for starch to develop "green" materials with controlled biodegradation rates to meet application needs. In this regard, research in still under way in our lab.

Acknowledgements

The research leading to these results has received funding from the Australian Research Council (ARC) under the Discovery Project 120100344. M. Li also would like to thank the China Scholarship Council (CSC), the Ministry of Education, P. R. China, for providing research funding for her PhD studies at The University of Queensland (UQ). The authors acknowledge the facilities, and the scientific and technical assistance, of the Australian Microscopy & Microanalysis Research Facility (AMMRF) at the Centre for Microscopy and Microanalysis (CMM), UQ.

References

Avérous, L. (2004). Biodegradable multiphase systems based on plasticized starch: a review. *Polymer Reviews, 44*(3), 231-274.

Biswas, A., Shogren, R. L., Stevenson, D. G., Willett, J. L., & Bhowmik, P. K. (2006). Ionic liquids as solvents for biopolymers: Acylation of starch and zein protein. *Carbohydrate Polymers, 66*(4), 546-550.

Bogracheva, T. Y., Wang, Y. L., & Hedley, C. L. (2001). The effect of water content on the ordered/disordered structures in starches. *Biopolymers, 58*(3), 247-259.

Cheetham, N. W. H., & Tao, L. (1998). Variation in crystalline type with amylose content in maize starch granules: an X-ray powder diffraction study. *Carbohydrate Polymers, 36*(4), 277-284.

Colquhoun, I. J., Parker, R., Ring, S. G., Sun, L., & Tang, H. R. (1995). An NMR spectroscopic characterisation of the enzyme-resistant residue from α-amylolysis of an amylose gel. *Carbohydrate Polymers, 27*(4), 255-259.

El Seoud, O. A., Koschella, A., Fidale, L. C., Dorn, S., & Heinze, T. (2007). Applications of ionic liquids in carbohydrate chemistry: A window of opportunities. *Biomacromolecules, 8*(9), 2629-2647.

Fu, Z.-q., Wang, L.-j., Li, D., Wei, Q., & Adhikari, B. (2011). Effects of high-pressure homogenization on the properties of starch-plasticizer dispersions and their films. *Carbohydrate Polymers, 86*(1), 202-207.

Jane, J.-l. (2009). Structural features of starch granules II. In B. James, & W. Roy (Eds.), *Starch (Third Edition)* (pp. 193-236). San Diego: Academic Press.

Kärkkäinen, J., Lappalainen, K., Joensuu, P., & Lajunen, M. (2011). HPLC-ELSD analysis of six starch species heat-dispersed in [BMIM]Cl ionic liquid. *Carbohydrate Polymers, 84*(1), 509-516.

Leroy, E., Jacquet, P., Coativy, G., Reguerre, A. l., & Lourdin, D. (2012). Compatibilization of starch–zein melt processed blends by an ionic liquid used as plasticizer. *Carbohydrate Polymers, 89*(3), 955-963.

Li, M., Liu, P., Zou, W., Yu, L., Xie, F., Pu, H., Liu, H., & Chen, L. (2011). Extrusion processing and characterization of edible starch films with different amylose contents. *Journal of Food Engineering, 106*(1), 95-101.

Liew, C.-W., Ramesh, S., Ramesh, K., & Arof, A. (2012). Preparation and characterization of lithium ion conducting ionic liquid-based biodegradable corn starch polymer electrolytes. *Journal of Solid State Electrochemistry, 16*(5), 1869-1875.

Liu, H., Xie, F., Yu, L., Chen, L., & Li, L. (2009). Thermal processing of starch-based polymers. *Progress in Polymer Science, 34*(12), 1348-1368.

Liu, P., Xie, F., Li, M., Liu, X., Yu, L., Halley, P. J., & Chen, L. (2011). Phase transitions of maize starches with different amylose contents in glycerol-water systems. *Carbohydrate Polymers, 85*(1), 180-187.

Liu, W., & Budtova, T. (2012). Dissolution of unmodified waxy starch in ionic liquid and solution rheological properties. *Carbohydrate Polymers, 93*(1), 199-206.

Lopez-Rubio, A., Flanagan, B. M., Gilbert, E. P., & Gidley, M. J. (2008). A novel approach for calculating starch crystallinity and its correlation with double helix content: A combined XRD and NMR study. *Biopolymers, 89*(9), 761-768.

Madrigal, L., Sandoval, A. J., & Müller, A. J. (2011). Effects of corn oil on glass transition temperatures of cassava starch. *Carbohydrate Polymers, 85*(4), 875-884.

Mateyawa, S., Xie, D. F., Truss, R. W., Halley, P. J., Nicholson, T. M., Shamshina, J. L., Rogers, R. D., Boehm, M. W., & McNally, T. (2013). Effect of the ionic liquid 1-ethyl-3-methylimidazolium

acetate on the phase transition of starch: Dissolution or gelatinization? *Carbohydrate Polymers, 94*(1), 520-530.

Perdomo, J., Cova, A., Sandoval, A. J., García, L., Laredo, E., & Müller, A. J. (2009). Glass transition temperatures and water sorption isotherms of cassava starch. *Carbohydrate Polymers, 76*(2), 305-313.

Pérez, S., Baldwin, P. M., & Gallant, D. J. (2009). Structural features of starch granules I. In B. James, & W. Roy (Eds.), *Starch (Third Edition)* (pp. 149-192). San Diego: Academic Press.

Pérez, S., & Bertoft, E. (2010). The molecular structures of starch components and their contribution to the architecture of starch granules: a comprehensive review. *Starch/Stärke, 62*(8), 389-420.

Ramesh, S., Liew, C.-W., & Arof, A. K. (2011). Ion conducting corn starch biopolymer electrolytes doped with ionic liquid 1-butyl-3-methylimidazolium hexafluorophosphate. *Journal of Non-Crystalline Solids, 357*(21), 3654-3660.

Ramesh, S., Shanti, R., Morris, E., & Durairaj, R. (2011). Utilisation of corn starch in production of 'green' polymer electrolytes. *Materials Research Innovations, 15*(1), s8.

Ramesh, S., Shanti, R., & Morris, E. (2012). Studies on the thermal behavior of CS:LiTFSI:[Amim] Cl polymer electrolytes exerted by different [Amim] Cl content. *Solid State Sciences, 14*(1), 182-186.

Sankri, A., Arhaliass, A., Dez, I., Gaumont, A. C., Grohens, Y., Lourdin, D., Pillin, I., Rolland-Sabaté, A., & Leroy, E. (2010). Thermoplastic starch plasticized by an ionic liquid. *Carbohydrate Polymers, 82*(2), 256-263.

Stevenson, D. G., Biswas, A., Jane, J.-l., & Inglett, G. E. (2007). Changes in structure and properties of starch of four botanical sources dispersed in the ionic liquid, 1-butyl-3-methylimidazolium chloride. *Carbohydrate Polymers, 67*(1), 21-31.

Tan, I., Flanagan, B. M., Halley, P. J., Whittaker, A. K., & Gidley, M. J. (2007). A method for estimating the nature and relative proportions of amorphous, single, and double-helical components in starch granules by ^{13}C CP/MAS NMR. *Biomacromolecules, 8*(3), 885-891.

Tang, H., & Hills, B. P. (2003). Use of ^{13}C MAS NMR to study domain structure and dynamics of polysaccharides in the native starch granules. *Biomacromolecules, 4*(5), 1269-1276.

Thuy Pham, T. P., Cho, C.-W., & Yun, Y.-S. (2010). Environmental fate and toxicity of ionic liquids: A review. *Water Research, 44*(2), 352-372.

van Soest, J. J. G., Hulleman, S. H. D., de Wit, D., & Vliegenthart, J. F. G. (1996). Crystallinity in starch bioplastics. *Industrial Crops and Products, 5*(1), 11-22.

Veregin, R. P., Fyfe, C. A., Marchessault, R. H., & Taylor, M. G. (1986). Characterization of the crystalline A and B starch polymorphs and investigation of starch crystallization by high-resolution carbon-13 CP/MAS NMR. *Macromolecules, 19*(4), 1030-1034.

Wang, J., Yu, L., Xie, F., Chen, L., Li, X., & Liu, H. (2010a). Rheological properties and phase transition of cornstarches with different amylose/amylopectin ratios under shear stress. *Starch/Stärke, 62*(12), 667-675.

Wang, N., Zhang, X., Liu, H., & He, B. (2009). 1-Allyl-3-methylimidazolium chloride plasticized-corn starch as solid biopolymer electrolytes. *Carbohydrate Polymers, 76*(3), 482-484.

Wang, N., Zhang, X., Wang, X., & Liu, H. (2009). Communications: Ionic liquids modified montmorillonite/thermoplastic starch nanocomposites as ionic conducting biopolymer. *Macromolecular Research, 17*(5), 285-288.

Wang, N., Zhang, X., Liu, H., & Han, N. (2010b). Ionically conducting polymers based on ionic liquid-plasticized starch containing lithium chloride. *Polymers & Polymer Composites, 18*(1), 53-58.

Way, C., Wu, D. Y., Dean, K., & Palombo, E. (2010). Design considerations for high-temperature respirometric biodegradation of polymers in compost. *Polymer Testing, 29*(1), 147-157.

Wilpiszewska, K., & Spychaj, T. (2011). Ionic liquids: Media for starch dissolution, plasticization and modification. *Carbohydrate Polymers, 86*(2), 424-428.

Xie, F., Halley, P. J., & Avérous, L. (2012). Rheology to understand and optimize processibility, structures and properties of starch polymeric materials. *Progress in Polymer Science, 37*(4), 595-623.

Xie, F., Liu, P., & Yu, L. (2014). Processing of plasticized starch-based materials: state of art and perspectives. In P. J. Halley, & L. R. Avérous (Eds.), *Starch Polymers: From Genetic Engineering to Green Applications* (pp. 257-289). Amsterdam, Boston, Heidelberg, London, New York, Oxford, Paris, San Diego, San Francisco, Singapore, Sydney, Tokyo: Elsevier.

Yu, L., Dean, K., & Li, L. (2006). Polymer blends and composites from renewable resources. *Progress in Polymer Science, 31*(6), 576-602.

Zakrzewska, M. E., Bogel-Łukasik, E., & Bogel-Łukasik, R. (2010). Solubility of carbohydrates in ionic liquids. *Energy & Fuels, 24*(2), 737-745.

Figure captions

Figure 1 SEM images of both normal and fracture surfaces of the different starch samples.

Figure 2 XRD patterns of native starch (Gelose 80) and the different starch samples.

Figure 3 ^{13C} CP/MAS and SPE/MAS NMR spectra of the sample I27 revealing the presence of [Emim][OAc] and amorphous starch in the SPE/MAS spectrum and the highly ordered material in the CP/MAS spectrum.

Figure 4 Tensile strength (σ) (top), Young's modulus (middle), and elongation at break (εb) (bottom) of the different starch samples. The errors bars represent standard deviations.

Figure 5 Tan δ results of the different starch samples.

Figure 6 TGA results in terms of weight percentage (a) and derivative weight percentage (b) of the different starch samples.

Tables

Table 1 Sample formulations, and the XRD, ^{13}C CP/MAS NMR and biodegradation results of the starch-based films

Code	Formulation[a]				XRD results (%)			NMR results (%)[b]					% Biodegradability (%)		
	Starch	Water	Glycerol	IL	B-type cryst. (±1)	V-type cryst. (±1)	Total cryst.	Double helix (±2)	Single helix (±1)	Total ordered	Rigid amorph. (±2)	Mobile amorph. (±2)	1 month	2 months	3 months
Native starch	–	–	–	–	33.7	ND[c]	33.7	–	–	–	–	–	–	–	–
Cellulose	–	–	–	–	–	–	–	–	–	–	–	–	77.4 (5)[d]	78.3 (<5)	79.9 (<5)
G9	100	21	9	0	26.6	5.5	32.1	28	4	32	40	28	68.6 (5)	76.2 (<5)	71.2 (7)
G18	100	12	18	0	21.8	5.6	27.4	20	7	27	43	30	74.0 (8)	82.5 (9)	86.8 (10)
G27	100	3	27	0	13.9	6.8	20.7	18	3	21	50	29	65.3 (10)	70.9 (8)	75.1 (9)
I9	100	21	0	9	18.0	6.1	24.1	13	11	24	52	24	34.1 (<5)	35.0 (<5)	39.0 (<5)
I18	100	12	0	18	16.6	4.6	21.2	14	7	21	44	35	13.7 (<5)	13.7 (<5)	14.3 (<5)
I27	100	3	0	27	14.7	2.5	17.2	14	3	17	24	59	16.7 (<5)	16.7 (<5)	16.7 (<5)

[a] Portions in weight; [b] Based on the assumption that the crystal defect fitting method for XRD (Lopez-Rubio et al., 2008) describes all the crystallinity present and the difference between the results from the XRD and NMR measurements is a result of the amorphous starch in the mobile phase; [c] Unable to be determined as the V-type crystallinity pattern was difficult to be differentiated from the B-type crystallinity pattern; [d] Standard deviation in the brackets.